GEOPHYSICAL RESEARCH LETTERS, VOL. 26, NO. 15, PAGES 2327-2330, AUGUST 1, 1999

Initial Measurements of the Lunar Induced Magnetic Dipole Moment Using Lunar Prospector Magnetometer Data

Lon L. Hood[1], David L. Mitchell[2], Robert P. Lin[2], Mario H. Acuna[3], Alan B. Binder [4]

Abstract. Twenty-one orbits of Lunar Prospector magnetometer data obtained during an extended passage of the Moon through a lobe of the geomagnetic tail in April 1998 are applied to estimate the residual lunar induced magnetic dipole moment. Editing and averaging of individual orbit segments yields a negative induced moment with amplitude $-2.4 \pm 1.6 \times 10^{22}$ Gauss-cm^3 per Gauss of applied field. Assuming that the induced field is caused entirely by electrical currents near the surface of a highly electrically conducting metallic core, the preferred core radius is 340±90 km. For an iron-rich composition, such a core would represent 1 to 3% of the lunar mass.

Introduction

The lunar induced magnetic dipole moment is a measure of the residual response of the lunar interior to a sudden exposure of the Moon to a spatially uniform magnetic field in a near-vacuum environment. A quantitative physical interpretation of the induced moment allows inferences to be drawn regarding properties of the interior that are sensitive to applied magnetic fields. In particular, if the induced moment can be attributed to the presence of a highly electrically conducting core, then the core radius may be inferred [*Goldstein and Russell*, 1975; *Goldstein et al.*, 1976; *Russell et al.*, 1981]. Conditions approaching a quasi-vacuum environment with the Moon exposed to a relatively steady, nearly uniform magnetic field occur for up to several days each month as the Moon traverses the north and/or south lobes of the geomagnetic tail. Within this low-density, relatively cold plasma environment, magnetic field changes parallel to the geomagnetic tail field result in induced fields external to the Moon that are comparable to those that would occur if the Moon were in a vacuum [*Hood and Schubert*, 1978].

During April of 1998, the Lunar Prospector orbit plane was nearly parallel to the Sun-Moon line and was therefore optimally oriented for detecting an induced moment in the geomagnetic tail (Figure 1). During the same month, the Moon entered the north tail lobe and remained there for an unusually long period (> 2 days) during which the tail lobe field was relatively strong and steady.

Data Analysis

Twenty-one orbits of Lunar Prospector magnetometer data were initially selected from an interval extending from approximately 0800 UT on April 9 to 1100 UT on April 11, 1998. During this period, the geotail field was oriented toward the Sun with an amplitude that varied randomly between limits of approximately 12 and 16 nT (1 nT = 1 nanoTesla = 10^{-5} Gauss). As an initial processing step, the measured field components in each orbit (approximately 1400 data points per orbit) were normalized to a common mean field amplitude of 14 nT and were transformed to a coordinate system de-

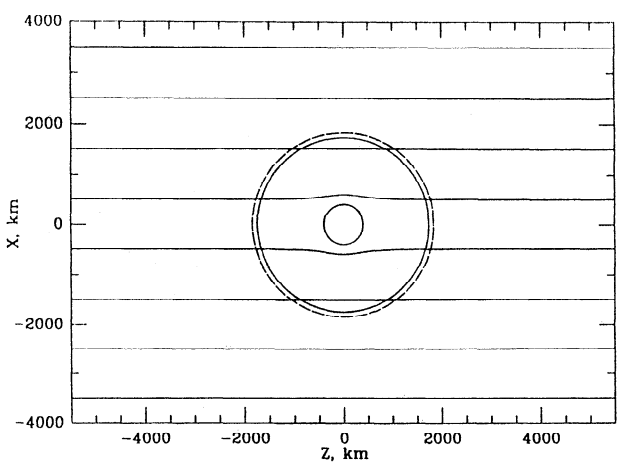

Figure 1. Perturbation of spatially uniform magnetic lines of force by an induced magnetic field caused by currents at the surface of a highly electrically conducting core of radius 400 km (inner circle). The outer solid circle represents the projection of the lunar surface and the outermost dashed circle indicates a nominal Lunar Prospector orbit at 100 km altitude. The orbit plane is parallel to the applied field orientation.

[1]Lunar and Planetary Laboratory, University of Arizona, Tucson, Arizona.

[2]Space Science Laboratory, University of California, Berkeley, CA.

[3]Goddard Space Flight Center, Greenbelt, MD.

[4]Lunar Research Institute, Gilroy, CA.

Paper number 1999GL900487.
0094-8276/99/1999GL900487$05.00

fined by the mean field orientation during that orbit (z is parallel to the applied field, y lies in the selenographic equatorial plane, and x completes the orthogonal system).

The z-component of the field (parallel to the geotail field) was characterized by especially large low-frequency transients and was therefore excluded from further consideration. The x- and y-components (perpendicular to the geotail field) were characterized by higher-frequency field fluctuations consisting of both external transients and permanent crustal fields. The mean rms deviations of these field fluctuations was near 1 nT for both the x- and y-components. For comparison, the field perturbation expected at the Lunar Prospector orbit altitude for a 400 km core and a 14 nT applied field is only $\sim$ 0.2 nT. Consequently, in order to reduce further the ambient noise level, several steps were taken. First, only those orbits and major orbit segments for each component having rms deviations less than 0.4 nT (6 to 7 orbits out of the original 21) were selected for further analysis as listed in Table 1. (Note that the selected intervals for each component do not necessarily coincide because the rms deviations can be lower in one component than in the other during a single orbit.) Second, short segments in some selected orbit intervals were deleted to minimize contributions from a large short-wavelength crustal field anomaly. Third, remaining external field fluctuations were minimized by averaging together all measurements ordered according to the time from the beginning of each orbit (chosen to coincide with the southward equatorial crossing time). Averaging over many orbits also helped to minimize fields resulting from electrical currents in the lunar mantle induced in response to random fluctuations of the geotail field (see next section).

The final mean x- and y-components of the field in the field-aligned system are plotted in Figure 2 after smoothing using a 51-point running mean algorithm. Representative standard deviations for individual average measurements are also shown. In the field-aligned system, y lies in the lunar equatorial plane and is perpendicular to the applied field direction, which is nearly parallel to the Sun-Moon line. y is therefore nearly perpendicular to the Lunar Prospector orbit plane while x is nearly parallel to this plane. From an inspection of Figure 1, almost no induced field should be present in the y-component while the x-component should contain nearly the entire induced field perturbation. For comparison, the long dashed line in Figure 2 shows the field perturbation expected for a moment of amplitude -3.2×10^{22} Gauss-cm^3 per Gauss of applied field (hereafter denoted G-cm^3/G). (The minus sign indicates that the moment is oriented opposite to the applied field.)

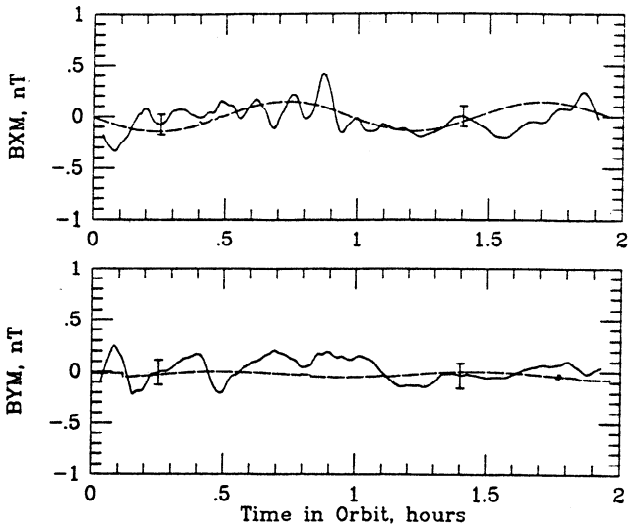

Figure 2. The irregular curves represent mean magnetic field perturbations in the x and y directions in the field-aligned system as calculated from the Lunar Prospector orbit segments listed in Table 1. The smooth dashed curves represent field perturbations expected for an induced magnetic moment of -3.2×10^{22} G-cm^3/G (equivalent core radius: 400 km).

Table 1. Selected Data Intervals

Field Comp.	Orbit #	Start Time Day No. Hour (UT)	End Time Day No. Hour (UT)	RMS
X	158	99, 19.9	99, 21.5	0.368
X	159	99, 21.5	99, 23.5	0.348
X	160	99, 23.5	100, 1.45	0.352
X	163	100, 5.7	100, 7.3	0.312
X	167	100, 13.5	100, 15.2	0.369
X	172	100, 23.4	100, 1.0	0.254
X	176	100, 6.9	101, 7.7	0.255
Y	160	99, 23.6	100, 1.5	0.338
Y	163	100, 6.2	100, 7.3	0.203
Y	166	100, 11.4	100, 12.1	0.223
Y	169	100, 17.7	100, 19.1	0.329
Y	173	101, 1.6	101, 3.0	0.224
Y	174	101, 3.0	101, 4.9	0.218

To investigate quantitatively whether the mean field perturbation data of Figure 2 imply a significant induced moment, theoretical field perturbations for induced moments of various amplitudes were fit to the data using a minimum-variance criterion. In all cases, the phase of the model field perturbation was kept constant since it is determined by the mean field orientation and direction, which are both known. Plotted in Figure 3 is the variance between the smoothed x-component measurements of Figure 2 and theoretical curves for a range of negative induced moments. Also shown on the horizontal scale of Figure 3 are the radii of highly electrically conducting cores assumed to be responsible for the negative induced moment (see next section). For example, an induced moment of -3.2×10^{22} G-cm^3/G corresponds to a metallic core radius of 400 km.

A shallow but distinct minimum variance in Figure 3 occurs for induced moments near -2×10^{22} G-cm^3/G. Moments with larger absolute magnitudes than 4×10^{22} G-cm^3/G are strongly excluded by the data while moments with smaller amplitudes than about 1×10^{22} G-cm^3/G are less strongly excluded. The depth of the variance minimum at 0.0153 nT^2 is 0.0036 nT^2 (23%)

below that for a core-free Moon. To test the significance of this x-component variance minimum, the same procedure was applied to the smoothed y-component data of Figure 2 which should (according to Figure 1) contain no induced field perturbation. The resulting variance curve is nearly flat for core radii less than 400 km and contains only a small minimum with a depth of 0.0016 nT^2. Thus, the long-wavelength perturbation is significantly larger in the x-component than in the y-component and produces a more distinct variance minimum with a depth of 0.0036 nT^2. Taking the depth of the y-component variance minimum (0.0016 nT^2) as an empirical measure of possible analysis errors (indicated by the horizontal dashed line in Figure 3), then the induced moment amplitude is in the range of -0.8 to -4×10^{22} G-cm^3/G and the corresponding core radius range is 250 to 430 km.

Interpretation

Induced magnetic fields may be either positive or negative, i.e., the induced moment may be either aligned with the applied field or oriented opposite to the applied field. A positive induced moment would result from paramagnetism of lunar mantle or crustal minerals or from a distribution of free metal. At depths greater than that of the Curie isotherm ($\sim$ 300 km), these effects are insignificant. The free metal content of crustal materials is negligible except in the case of near-surface breccias and soils. Paramagnetic effects should therefore mainly arise from paramagnetism of minerals in the lunar upper mantle and crust. For example, orthopyroxene with a Mg number of 75 has a bulk permeability of 1.001. Assuming that only the outer 300 km of the Moon contributes to any positive induced moment, the resulting amplitude would be of the order of $+1$–2×10^{21} G-cm^3/G, less than 10% of the negative induced moment estimated from Figure 3. We therefore neglect paramagnetism effects here.

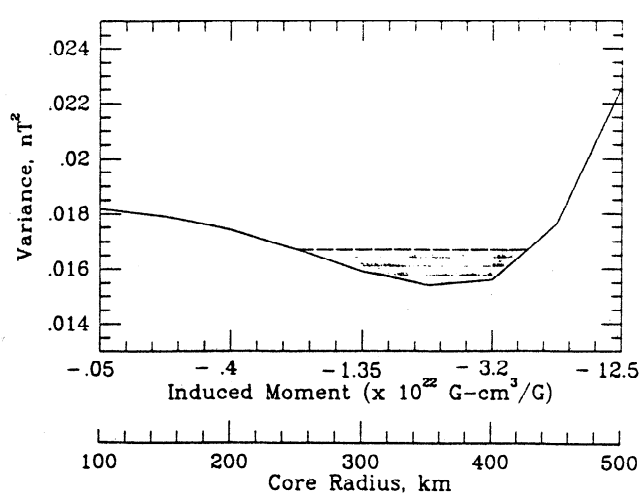

Figure 3. Variances of model x-component field perturbations from observed mean field perturbations as a function of induced moment amplitude and equivalent core radii. The dashed line and shaded region indicates the estimated range of uncertainty in the inferred moment amplitude.

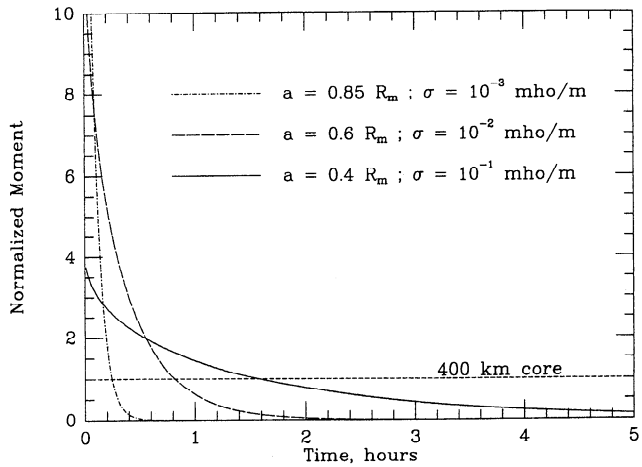

Figure 4. Each curve represents the temporal decay of an induced magnetic dipole moment for a sphere of the indicated radius and conductivity. Moments are normalized to that of a perfectly conducting core with radius 400 km.

A negative induced moment results from electrical currents flowing in the lunar mantle and core that, according to Faraday's Law, oppose any external magnetic field change. After application of an applied field (e.g., the geotail field), currents are initially induced in the weakly conducting lunar mantle as the external field change diffuses into the interior. If a highly electrically conducting core is present, a residual induced moment will be detected owing to currents near the surface of the core after all mantle currents have decayed.

The rate of decay of mantle currents may be estimated to first order from an analytic expression for the induced moment m_i produced by a constant-conductivity sphere of radius a and conductivity σ:

$$m_i = -\frac{1}{2}B_o a^3\left(\frac{6}{\pi^2}\right)\sum_{n=1}^{\infty}[\exp(-n^2\pi^2 t/\gamma)]/n^2$$

where $\gamma = 4\pi\sigma a^2/c^2$ (c is the speed of light) and B_o is the amplitude of the applied field. Here, σ is in Gaussian units of $\sec^{-1} = 9 \times 10^9$ mho/m. For $t = 0$, the summation has the value $\pi^2/6$; therefore, the induced moment has the initial value $\frac{1}{2}B_o a^3$ regardless of the value of σ. Limits on electrical conductivity as a function of depth in the lunar mantle have been previously estimated from time-dependent induction studies using Apollo data. A summary of available limits derived by several different groups is given in Figure 13 of *Hood et al.* [1982]. From these results, we estimate $\sigma \simeq 10^{-3}$ mho/m for $0.6 < r < 0.85$ R_m (1 R_m = 1738 km); $\sigma \simeq 10^{-2}$ mho/m for $0.4 < r < 0.6$ R_m; and $\sigma = 10^{-1}$ mho/m for $r < 0.4$ R_m. The electrical conductivity of metallic iron is many orders of magnitude larger than this and is effectively infinite for the time scales of interest here. Shown in Figure 4 are plots of the induced moment amplitude versus time for constant-conductivity spheres corresponding to the mantle layers defined above. The induced moments are expressed in terms of the residual moment for a perfectly conducting core of radius 400 km. In the case of the outermost con-

ducting sphere with $a = 0.85\ R_m$ and $\sigma = 10^{-3}$ mho/m, the induced field is initially large but decays rapidly in less than an hour to values much less than that of the core. In the case of the second sphere with $a = 0.6\ R_m$ and $\sigma = 10^{-2}$ mho/m, the induced field also decays within a period of about 2 hours. In the case of the innermost sphere with $a = 0.4\ R_m$ and $\sigma = 10^{-1}$ mho/m, the induced field persists until at least 5 hours after application of the applied field. Although a more accurate calculation would require a more complex model with multiple conductivity layers, this simplified calculation with constant conductivity spheres is sufficient to estimate that the time period required for the decay of mantle induced fields is about five hours. For comparison, the induced moment measurements of the previous section were obtained during a tail lobe pass with a duration of several days. During this period, the tail lobe field had a nearly constant (sunward) orientation and an amplitude that varied slowly between 12 and 16 nT. The resulting induced moment measurements should therefore be representative of the core induced moment.

Discussion

Based on the above analysis of a single lunar tail lobe pass, a negative induced moment of $-2.4 \pm 1.6 \times 10^{22}$ G-cm^3/G is estimated. This estimated moment derived from Lunar Prospector data is marginally consistent with an earlier estimate of $-4.2 \pm 0.6 \times 10^{22}$ G-cm^3/G derived from Apollo subsatellite geotail magnetometer data [*Russell et al.*, 1981], when the errors of both analyses are considered. It is also consistent with an upper bound of 435 km for the core radius derived by C. P. Sonett and collaborators from Apollo surface and orbital magnetometer data when the Moon was in the solar wind and terrestrial magnetosheath [*Hobbs et al.*, 1983]. Further studies of additional lunar tail lobe passes may refine and test this estimate further. Opportunities for induced moment measurements occur at $\sim$ 6 month intervals as the Lunar Prospector orbit plane passes near to the Sun-Moon line.

As concluded in the previous section, a possible and reasonable interpretation of the present induced moment measurement is that the mean applied field in the geotail during the April 1998 tail lobe pass was excluded for a protracted period by a highly electrically conducting lunar core. In principle, a fully molten silicate core (conductivity $\sim$ 10 mho/m) could also produce such a residual moment. However, it is theoretically difficult to maintain a large reservoir of silicate melt in the lunar interior in the presence of subsolidus convection early in lunar history. A metallic core with radius 340 $\pm$ 90 km is therefore suggested as a plausible interpretation. A small dense core has been independently indicated by lunar evolutionary models combined with the observationally derived normalized moment of inertia [*Konopliv et al.*, 1999; *Hood and Jones*, 1987]. Continued analysis of lunar laser ranging data has also yielded dynamical evidence for a fluid metallic core with a radius in the range of 300–375 km [*Williams et al.*, 1999]. These inferences should be tested with future geophysical data acquisition, preferably by surface seismometers [*Mizutani*, 1998].

Acknowledgments. The Lunar Prospector Program is funded by contract from NASA Ames to Lockheed-Martin. We especially thank David Curtis for his work with the ER and MAG instruments.

References

Goldstein, B. E., R. J. Phillips, and C. T. Russell, Magnetic permeability measurements and a lunar core, *Geophys. Res. Lett., 3*, 289-292, 1976.

Goldstein, B. E., and C. T. Russell, On the apparent diamagnetism of the lunar environment in the geomagnetic tail lobes, *Proc. Lunar Sci. Conf. 6th; Geochim. Cosmochim. Acta, Suppl. 6*, Houston, pp. 2999-3012, 1975.

Hobbs, B. A., L. L. Hood, F. Herbert, and C. P. Sonett, An upper bound on the radius of a highly electrically conducting lunar core, *Proc. Lunar Planet. Sci. Conf. 14th, J. Geophys. Res., 88, supplement*, p. B97-B102, 1983.

Hood, L. L., F. Herbert, and C. P. Sonett, The deep lunar electrical conductivity profile: Structural and thermal inferences, *J. Geophys. Res., 87*, 5311-5326, 1982.

Hood, L. L. and J. Jones, Geophysical constraints on lunar bulk composition and structure: A reassessment, Proc. 17th Lunar Planet. Sci. Conf., J. Geophys. Res., 92, E396-E410, 1987.

Hood, L. L. and G. Schubert, A magnetohydrodynamic theory for the lunar response to time variations in a spatially uniform ambient magnetic field, in *Proc. Lunar Planet. Sci. Conf. 9th*, 3125-3135, Lunar and Planetary Institute, Houston, 1978.

Konopliv, A., A. Binder, L. L. Hood, A. Kucinskas, W. L. Sjogren, and J. G. Williams, Improved gravity field of the Moon from Lunar Prospector, *Science, 281*, 1476-1480, 1998.

Mizutani, H., Lunar interior exploration by Japanese Lunar Penetrator Mission, LUNAR-A, *J. Phys. Earth, 43*, 657-670, 1998.

Russell, C. T., B. E. Goldstein, and P. J. Coleman, Jr., Magnetic evidence for a lunar core, *Proc. Lunar Planet. Sci. Conf. 12th*, 831-836, 1981.

Williams, J. G., D. H. Boggs, J. T. Ratcliff, and J. O. Dickey, The Moon's molten core and tidal Q, (abstract), Lunar and Planetary Science XXX, Lunar and Planetary Institute, Houston.

Lon L. Hood, Lunar and Planetary Laboratory, University of Arizona, Tucson, AZ, 85721-0092.

David L. Mitchell and Robert P. Lin, Space Science Laboratory, University of California, Berkeley, CA, 94720-7450.

Mario H. Acuna, Goddard Space Flight Center, Greenbelt, MD, 20771.

Alan B. Binder, Lunar Research Institute, Gilroy, CA, 95020.

(Received February 1, 1999; revised April 2, 1999; accepted May 28, 1999.)